Journal of Alzheimer's Disease 45 (2015) 45–56
DOI 10.3233/JAD-141659
IOS Press

Retinal Ganglion Cell Analysis Using High-Definition Optical Coherence Tomography in Patients with Mild Cognitive Impairment and Alzheimer's Disease

Carol Yim-lui Cheung[a,b,c,1,*], Yi Ting Ong[a,b,d,1], Saima Hilal[b,e,h], M. Kamran Ikram[a,b,c,e], Sally Low[a], Yi Lin Ong[a], N. Venketasubramanian[e], Philip Yap[f], Dennis Seow[g], Christopher Li Hsian Chen[e,h,2] and Tien Yin Wong[a,b,c,2]

[a]*Singapore Eye Research Institute, Singapore National Eye Centre, Singapore*
[b]*Department of Ophthalmology, Yong Loo Lin School of Medicine, National University of Singapore, Singapore*
[c]*Office of Clinical Sciences, Duke-NUS Graduate Medical School, Singapore*
[d]*NUS Graduate School for Integrative Sciences and Engineering, National University of Singapore, Singapore*
[e]*Memory Aging and Cognition Centre, National University Health System, Singapore*
[f]*Department of Geriatric Medicine, Khoo Teck Puat Hospital, Singapore*
[g]*Department of Geriatric Medicine, Singapore General Hospital, Singapore*
[h]*Department of Pharmacology, National University of Singapore, Singapore*

Accepted 11 November 2014

Abstract.
Background: Alzheimer's disease (AD) is a neurodegenerative disorder with emerging evidence that it is associated with retinal ganglion cell loss; however, few data exist to establish this association.
Objective: To determine whether macular ganglion cell-inner plexiform layer (GC-IPL) and retinal nerve fiber layer (RNFL), as quantitatively measured by non-invasive *in vivo* spectral-domain optical coherence tomography (SD-OCT), are altered in patients with AD and mild cognitive impairment (MCI).
Methods: Patients with AD and MCI were recruited from dementia/memory clinics, and cognitively normal controls were selected from the Singapore Epidemiology of Eye Disease program. SD-OCT (Cirrus HD-OCT, software version 6.0.2, Carl Zeiss Meditec Inc, Dublin, CA) was used to measure the GC-IPL and RNFL thicknesses.
Results: Compared with cognitively normal controls ($n = 123$), patients with AD ($n = 100$) had significantly reduced GC-IPL thicknesses in all six (superior, superonasal, inferonasal, inferior, inferotemporal, and superotemporal) sectors (mean differences from -3.42 to -4.99 μm, all $p < 0.05$) and reduced RNFL thickness in superior quadrant (-6.04 μm, $p = 0.039$). Patients with MCI ($n = 41$) also had significantly reduced GC-IPL thicknesses compared with controls (mean differences from -3.62 to -5.83 μm, all $p < 0.05$). Area under receiver operating characteristic curves of GC-IPL were generally higher than that of RNFL to discriminate AD and MCI from the controls.
Conclusions: Our data strengthens the link between retinal ganglion cell neuronal and optic nerve axonal loss with AD, and suggest that assessment of macular GC-IPL can be a test to detect neuronal injury in early AD and MCI.

Keywords: Alzheimer's disease, mild cognitive impairment, neurodegenerative disorder, optic nerve, retinal ganglion cell, spectral-domain optical coherence tomography

[1]These authors contributed equally to this work as first authors.

[2]These authors contributed equally to the work as last authors.

*Correspondence to: Dr. Carol Y. Cheung, Singapore Eye Research Institute, The Academia, 20 College Road, Discovery Tower Level 6, Singapore 169856. Tel.: +65 6576 7233; E-mail: carol.cheung.y.l@seri.com.sg.

INTRODUCTION

Alzheimer's disease (AD), the most common form of dementia, is associated with a specific pattern of pathological changes in the brain that result in neurodegeneration and the progressive development of dementia [1]. The hippocampus and entorhinal cortex have consistently demonstrated early neuronal damage in AD, but the detection of early changes *in vivo* in these areas is problematic [2, 3].

The retina develops as an extension of the central nervous system and shares similar embryological, anatomical, and physiological properties with the cerebral neurons, offering a possible "window" to study neurodegenerative disorder *in vivo* [4, 5]. Previous histological studies have demonstrated that patients with AD have loss of retinal ganglion cells (RGCs) and optic nerve axons [6–8]. Moreover, a few clinical studies have reported changes in optic nerve head (e.g., increased cup-to-disc ratio), observed clinically or using retinal photography, among AD patients [9, 10]. However, the clinical usefulness of optic nerve head evaluation is limited, due to high inter-observer variability in such assessment particularly the subtle changes of the optic nerve [9].

Optical coherence tomography (OCT) is a noninvasive *in vivo* optical biopsy and cellular-resolution imaging technology based on the principle of low-coherence interferometry, and has made remarkable advances in assessing optic nerve axons quantitatively in the last two decades, particularly for the diagnosis of glaucoma [11, 12]. Several studies have used OCT to assess peripapillary retinal nerve fiber layer (RNFL) thickness in AD and reported RNFL reduction in AD patients compared with normal controls [13–19].

Importantly, improved spatial resolution of spectral-domain OCT (SD-OCT) now allows measurement of the RGC layer composed of cell bodies; and the inner plexiform layer containing the RGC dendrites, and hence more detailed assessment of RGCs in the macular region [20, 21]. Since the macula contains more than 50% of total RGCs and that RGC cell body size is 10 to 20 times the diameter of their axons, we hypothesize that changes in the ganglion cell-inner plexiform layer (GC-IPL) thickness at the macula will be more sensitive than RNFL axonal reduction to neurodegenerative processes. In this study, we examined the associations of macular GC-IPL and RNFL thicknesses, as measured by SD-OCT, with AD and mild cognitive impairment (MCI).

MATERIALS AND METHODS

Study population

Patients

We conducted a case-control study of AD and MCI patients compared with controls selected from a population-based study of eye disease in Singapore. AD and MCI patients were enrolled consecutively from July 2009 to May 2013 from three study sites (dementia/memory clinics from the National University Hospital, Khoo Teck Puat Hospital, and Singapore General Hospital, Singapore). All patients underwent clinical and neuropsychiatric assessment. Computed tomography or MRI was reviewed as part of the diagnostic process. AD patients fulfilled Diagnostic and Statistical Manual of Mental Disorders, 4th edition (DSM-IV) criteria for dementia syndrome (Alzheimer's type) [22] and National Institute of Neurological and Communicative Disorders and Stroke and the Alzheimer's Disease and Related Disorders Association (NINDS-ADRDA) criteria for probable or possible AD [23]. Diagnosis of MCI was in accordance to Petersen et al.'s criteria [24]. We excluded patients with a history of glaucoma and presence of glaucomatous characteristics from fundus photographs. Presence of cataract, diabetic retinopathy, and maculopathy were not part of exclusion criteria, unless the pathologies affected the SD-OCT image quality (signal strength less than 5) or there was presence of GC-IPL or RNFL algorithm segmentation failure.

Controls

Cognitively normal controls were selected from a population-based study, the Singapore Chinese Eye Study (SCES). The methodology and objectives of the study population are reported in detail elsewhere [25, 26]. SCES participants aged 60 years or above were administered the Abbreviated Mental Test (AMT) for assessment of cognitive function. The AMT is a 10-question cognitive screening instrument (with minimum score of 0 and maximum score of 10), which has been modified for the local Singapore context and validated [27]. All the selected controls had normal AMT results, no history of stroke ascertained from self-report, no glaucomatous characteristics from fundus examination, and had a reliable and normal visual field (without a visual field defect).

Written, informed consent was obtained from each participant; the study conducted adhered to the

Declaration of Helsinki. Ethical approval was obtained from the Singapore Eye Research Institute Institutional Review Board and National Healthcare Group Pte Ltd Domain Specific Review Board.

SD-OCT imaging

The Cirrus HD-OCT (Carl Zeiss Meditec, Inc., Dublin, CA) is a commercially available SD-OCT device with a scan speed of 27,000 axial scans per second and an axial resolution of 5 μm [28]. Fig. 1 shows detailed retinal layers of a cross-sectional SD-OCT image centered at the macula from a human subject. After pupil dilation using tropicamide 1% and phenylephrine hydrochloride 2.5%, Cirrus HD-OCT was used to acquire one macular scan and one optic disc scan using the macular cube 200 × 200 and optic nerve head cube 200 × 200 scan protocols respectively in each eye. Re-scanning was performed if a motion artefact (indicated by blood vessels discontinuity) or saccades were detected. All the OCT scans included in the study had signal strength of at least 5. All scans were visually inspected by a trained grader masked to subject characteristics for quality check before inclusion into the study. OCT scans were excluded in the presence of motion artefacts, or GC-IPL or RNFL algorithm segmentation failure due to any retinal pathology (e.g., age-related macular degeneration, diabetic retinopathy, epiretinal membrane, macular hole). Patients with at least one type of scan with gradable quality were included for analysis. Of the cases, 20 patients were excluded. Among these 20 patients, 8 were excluded due to macular pathology affecting GC-IPL and RNFL segmentation algorithm (four epiretinal membrane, one age-related macular degeneration, two myopic pathology, one diabetic macular edema). The remaining 12 were excluded due to poor image quality (primarily motion artefacts due to poor fixation) on both macular and optic disc scans. Details of the Cirrus HD-OCT macular and optic disc scan protocols have been described in detail elsewhere [20, 25].

With the latest software version (Cirrus HD-OCT, software version 6.0.2, Carl Zeiss Meditec, Dublin, CA), a series of GC-IPL parameters (average, superior, superonasal, inferonasal, inferior, inferotemporal, superotemporal sectors) from macular cube are derived automatically. The software detects and measures the GC-IPL thicknesses automatically within a 14.13 mm^2 elliptical annulus area centered on the fovea from 3-dimensionals. The annulus has an inner vertical diameter of 1 mm and an outer diameter of 4 mm, and an inner horizontal diameter of 1.2 mm and an outer diameter of 4.8 mm. The size of the inner ring was chosen so as to exclude the area wherein the macular GC-IPL is very thin and difficult to detect accurately, whereas the dimensions of the outer ring were selected so as to include the area wherein the macular GC-IPL is thickest in a normal eye. The ganglion cell analysis algorithm detects the outer boundary of the RNFL as well as the outer boundaries yields

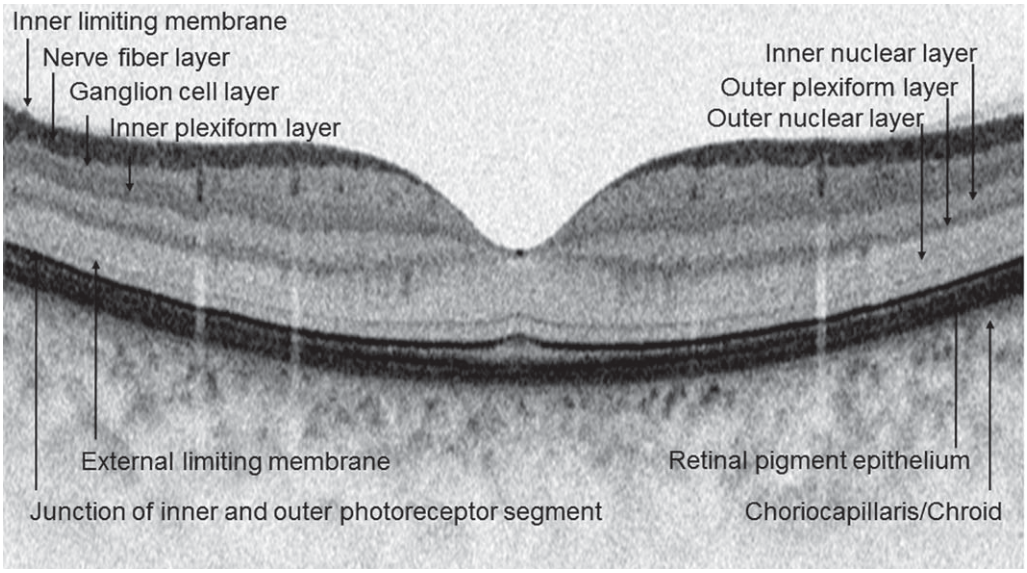

Fig. 1. Detailed retinal layers of a cross-sectional spectral-domain optical coherence topography image centered at the macula from a human subject.

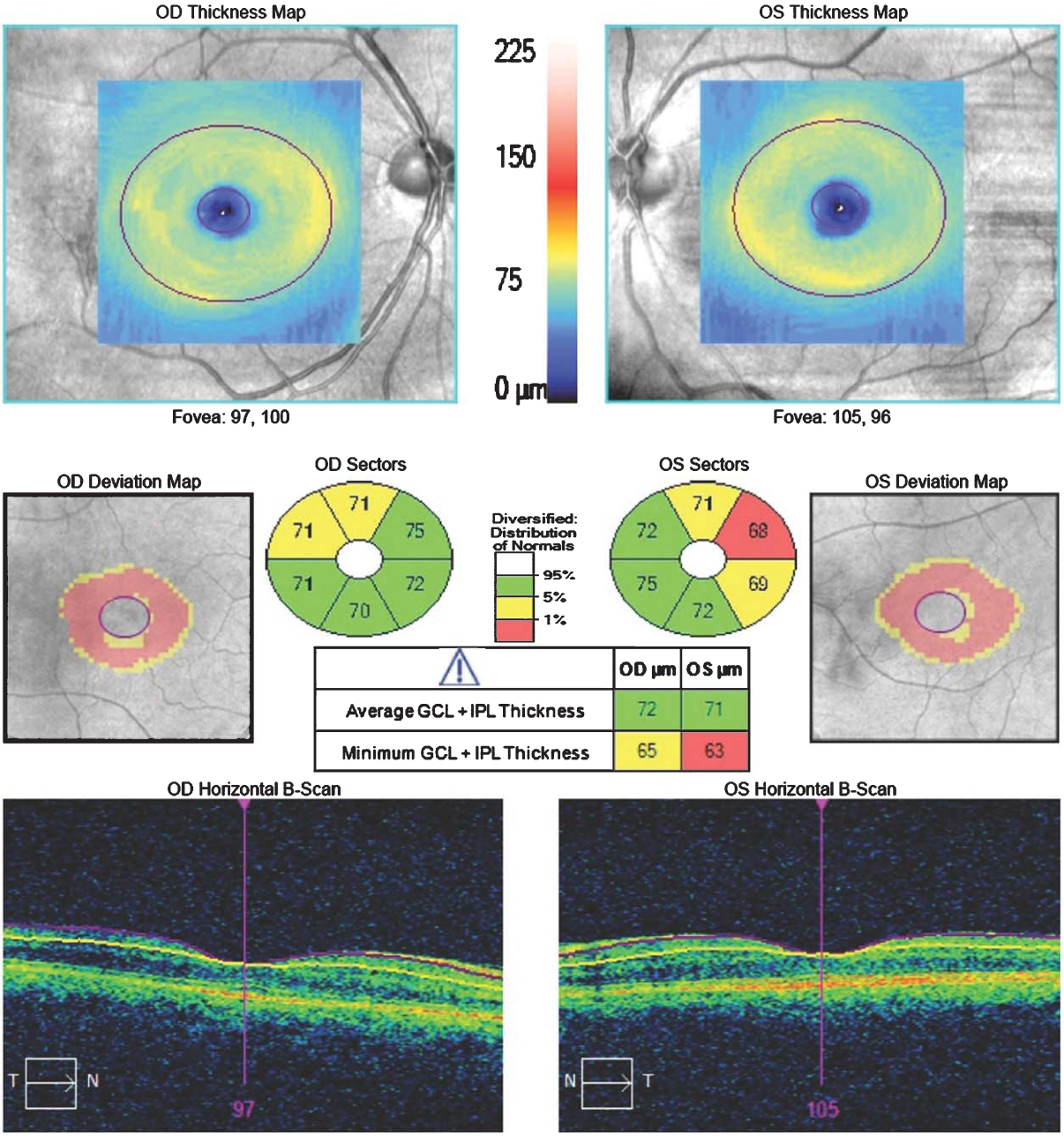

Fig. 2. An output of the Cirrus HD-OCT ganglion cell analysis (GCA) algorithm (Carl Zeiss Meditec, Dublin, CA) in a MCI subject. The GC-IPL thickness map uses a false color coding with warm colors representing high and cool colors representing low GC-IPL thickness values. The GC-IPL thickness map has a central circular black area expressing the lack of RGCs in the fovea. In MCI, RGC loss and, thus, GC-IPL reduction is expressed by the fading of warm colors and the appearance of more light blue areas. The software further compares the measured thickness to the device's internal normative age-matched database, generating a deviation map and a significance map color-coded to match GC-IPL thickness, with values within the normal range in green ($p = 5\%–95\%$), borderline values in yellow ($1\% < p < 5\%$), and values outside the normal range in red ($p < 1\%$). A super-pixel is shown in red or yellow in the deviation map if the GC-IPL thickness value falls outside the 99% or within 95%–99% centile range, respectively. Numeric values in sectors represent average GC-IPL thickness in the corresponding sector.

the combined thickness of the GCL and the IPL [29]. Fig. 2 shows an output of the Cirrus HD-OCT ganglion cell analysis algorithm in a MCI subject. Significant GC-IPL reduction was observed from deviation and thickness maps, compared with the built-in normative database.

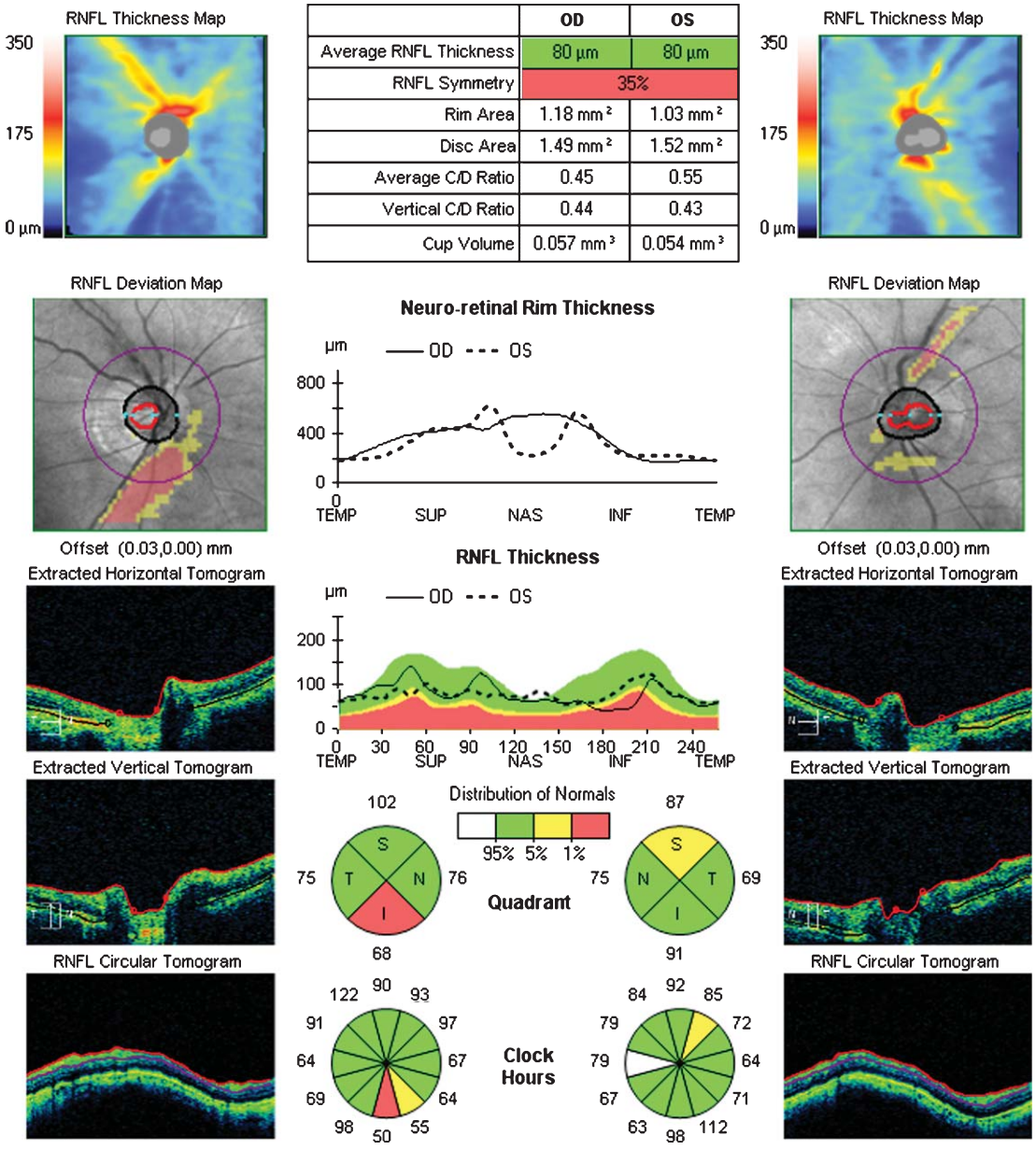

Fig. 3. An output of the Cirrus HD-OCT optic nerve head (ONH) algorithm (Carl Zeiss Meditec, Dublin, CA) in an AD subject. The RNFL thickness map uses a false color coding with warm colors representing high and cool colors representing low RNFL thickness values. In AD, RNFL loss and, thus, RNFL reduction is expressed by the fading of warm colors and the appearance of more light blue areas. The software further compares the measured thickness to the device's internal normative age-matched database, generating a deviation map, and a significance map color-coded to match RNFL thickness, with values within the normal range in green ($p = 5\%$–95%), borderline values in yellow ($1\% < p < 5\%$), and values outside the normal range in red ($p < 1\%$). A super-pixel is shown in red or yellow in the deviation map if the RNFL thickness value falls outside the 99% or within 95%–99% centile range, respectively. Numeric values outside sectors represent average RNFL thickness in the corresponding sector.

A series of peripapillary RNFL thicknesses (e.g., average, superior quadrant, nasal quadrant, inferior quadrant, and temporal quadrant) was derived automatically from optic nerve head cube. The built-in algorithm automatically detected the optic disc center and positioned a calculation circle of diameter 3.46 mm around the optic disc on the RNFL thickness map. Clock hour, quadrant, and average RNFL thicknesses were derived from the calculation circle and displayed in the analysis printout. Fig. 3 shows an

output of the Cirrus HD-OCT optic nerve head analysis algorithm in an AD patient. Significant RNFL reduction was observed from deviation and thickness maps, compared with the built-in normative database.

Other variables

AD and MCI patients were categorized into three groups based on Clinical Dementia Rating global scores at admission into the study. Years since first cognitive symptom to date of admission into study were also calculated. Self-reported history of systemic diseases (hypertension, hypercholesterolemia, diabetes mellitus) and medication use were elicited from the patient and their primary caregiver at the study interview. Smoking was defined as those currently smoking any number of cigarettes (i.e., current versus past/never). Previous myocardial infarction was ascertained from self-report.

Statistical analysis

All statistical analyses were performed using SPSS statistics version 21.0 and R version 3.1.1 (The R foundation for statistical computing). We selected one eye from each participant randomly for final analysis. Analyses of variance (ANOVA), chi-squared test, and Wilcoxon rank-sum test were used to compare the characteristics among the groups (AD, MCI, and controls) in the study. We then used analyses of covariance (ANCOVA) to estimate mean GC-IPL and RNFL thicknesses in the groups adjusted for age, gender, ethnicity, SD-OCT signal strength (Model 1) and additionally adjusted for optic disc areas (only for the models of RNFL), hypertension, diabetes and, history of myocardial infarction (Model 2). Area under receiver operating characteristic curves (AUCs) was used to assess the ability of GC-IPL and RNFL thicknesses to discriminate AD, MCI, and AD/MCI from cognitively normal controls adjusting for age and gender.

RESULTS

We included 100 AD patients, 41 MCI patients, and 123 cognitively normal subjects in the final analysis. Table 1 shows the characteristics of the AD, MCI, and control groups. AD and MCI patients were older, more likely to be female, hypertensive, diabetic, and had history of myocardial infarction, but had lower blood pressure measures, compared with the cognitively normal control subjects.

Table 2 shows the relationship of GC-IPL thicknesses with AD, MCI, and cognitively normal control groups. GC-IPL thickness showed significant reduction across all groups in all the sectors (all p-values ≤ 0.016). Compared with the cognitively normal controls, AD patients had significantly reduced GC-IPL thicknesses in all the sectors after adjusting for age, gender, ethnicity, SD-OCT signal strength, hypertension, diabetes, and history of myocardial infarction (both Models 1 & 2). MCI patients also had significantly reduced GC-IPL thicknesses in the majority of sectors compared with cognitively normal controls (except in superotemporal sector in Model 1). The associations of MCI in superior and inferionasal sectors were attenuated after additional adjustment for hypertension, diabetes, and history of myocardial infarction (Model 2). There were no significant differences in GC-IPL thickness between AD and MCI. Additional adjustment with age^2 or restricting analysis to only Chinese cases and controls yielded similar results.

Table 3 shows the relationship of RNFL thicknesses between the AD, MCI, and cognitively normal control groups. RNFL thickness showed significant reduction across the groups in average, superior, and inferior quadrants in Model 1, but this was only statistically significant in the superior quadrant in Model 2. Compared with the cognitively normal controls, the AD patients had significantly reduced average, superior, and inferior RNFL thicknesses, but the associations were attenuated in average and inferior quadrant in Model 2. There were no significant differences in RNFL thickness between MCI and controls, and AD and MCI. Results for both RNFL and GC-IPL remained largely similar when persons with diabetes were excluded.

Table 4 shows the AUCs of GC-IPL and RNFL thicknesses to discriminate AD, MCI, and AD/MCI from cognitively normal controls, adjusted for age and gender. Among the GC-IPL parameters, the AUC of inferior sector had highest value to discriminate AD and AD/MCI from cognitively normal controls, while the AUC of inferotemporal sector had highest value to discriminate MCI from cognitively normal controls.

DISCUSSION

In this study, we demonstrate that macular GC-IPL and peripapillary RNFL reduction, as assessed by SD-OCT, is strongly related to AD, strengthening the link between RGC neuronal and optic nerve axonal loss with neurodegenerative disorders such as AD.

Table 1
Characteristics of Alzheimer's disease (AD) cases, mild cognitive impairment (MCI) cases, and cognitively normal controls in the study

	AD ($n = 100$)	MCI ($n = 41$)	Controls ($n = 123$)	p-value
Gender (Male/Female)	43/57	13/28	67/56	0.027
Race (Chinese/Malay/Indian)	79/15/6	29/3/9	123/0/0	<0.001
Clinical Dementia Rating global score 0–0.5/1/2–3	0/77/22	41/0/0	–	<0.001
	Mean (SD)	Mean (SD)	Mean (SD)	
Years since first cognitive symptom	3.1 (2.4)	2.2 (1.4)	–	0.033
Age, years	73.5 (6.23)	70.4 (10.2)	65.7 (3.77)	<0.001
Systolic blood pressure, mmHg	133.0 (19.3)	136.5 (20.9)	139.9 (17.2)	0.027
Diastolic blood pressure, mmHg	70.0 (10.8)	71.2 (10.3)	77.4 (9.14)	<0.001
	%	%	%	
Smoking (current versus past/never)	9.0	9.8	11.4	0.838
Hypertension	82.0	58.5	40.7	<0.001
Diabetes	47.0	17.1	13.0	<0.001
Hypercholesterolemia	63.0	63.4	52.8	0.240
History of myocardial infarction	13.0	9.8	2.4	0.010

p values were calculated by ANOVA for continuous, chi-square for categorical data, and Wilcoxon rank-sum test for years since onset.

RGCs, the neurons located in the GCL in the retina, become myelinated when they leave the eyes, forming the optic nerve and providing the connection between the eye and the central nervous system [30]. With rapid advancements in OCT technology, more detailed and precise quantitative assessment of retinal neuronal and axonal neurodegenerative pathologies can now be performed using SD-OCT. We now show that patients with AD have macular GC-IPL and peripapillary RNFL reduction, as measured by SD-OCT. This is consistent with previous histological studies [6–8] and animal studies [31, 32], supporting the hypothesis that changes in RGCs and optic nerve axons reflect neurodegenerative pathology in AD. Our findings were also consistent with previous clinical studies showing that reduced RNFL thickness, particularly in the superior quadrant, measured by less sensitive time-domain OCT, is observed in AD patients [13–18].

Second, we found that macular GC-IPL neuronal loss is more strongly related to MCI, compared with RNFL axonal loss, suggesting that RGC neuronal loss might begin in the macula because of the dense population of RGCs in this region. Macular GC-IPL, a new SD-OCT parameter that reflects the thickness of RGC bodies and dendrites in the retina, is based on a sampling of approximately 50% of the RGC population whose bodies are more than 10 to 20 times the diameter of their axons [33]. Blanks et al. previously demonstrated substantial loss of RGCs in the foveal/parafoveal region in AD in a postmortem study [34]. Furthermore, RGC dendrites are confined to the IPL of the retina. There is increasing evidence that in neurodegenerative conditions, morphological alterations of dendrites (e.g., reduction in dendritic length and branches) occurs both in the retina and in the central nervous system [30]. In addition, Williams et al. recently reported that RGC dendritic changes precede cell loss in a mouse model of AD, suggesting that the IPL may be a useful marker for the early detection of AD-related neurodegeneration [35]. Therefore, it is reasonable to speculate that GC-IPL thickness is a more sensitive marker than RNFL thickness for assessing neurodegeneration pathology in MCI or early AD.

To our knowledge, there is only one other study which has analyzed the association between GCL, measured by SD-OCT, in AD patients. Marziani et al. reported significant reductions in combined RNFL and GCL thickness (RNFL+GCL) in macular region assessed by another SD-OCT (Spectralis SD-OCT, Heidelberg Engineering, Heidelberg, Germany) in 21 AD patients compared with healthy controls [36]. Nevertheless, RGCs structure differs less in a normal population than RNFL, hence including the RNFL in the ganglion cell analysis in the macular region may affect the sensitivity for detecting ganglion cell abnormalities [29]. Our study importantly measured the GC-IPL without including the RNFL using the latest SD-OCT ganglion cell analysis algorithm, which is less influenced by RNFL thickness variation than macular ganglion cell complex thickness (includes RNFL, GCL, and IPL) [29].

AD, the most common cause of dementia, is a major public health problem [37, 38], hence there is a pressing need to develop sensitive markers that may serve as adjuncts to current clinical and neuropsychological tests for early recognition of AD and for facilitating early-intervention studies to prevent or slow disease progression. We proposed that RGCs loss may be a biomarker of neuronal degeneration in AD and assessment of RGCs neuronal and axonal degeneration (GC-

Table 2
Relationship of ganglion cell-inner plexiform layer (GC-IPL) thickness with Alzheimer's disease (AD) and mild cognitive impairment (MCI)

GC-IPL thickness	AD ($n=99$)	MCI ($n=41$)	Controls ($n=123$)		AD versus Controls		MCI versus Controls		AD versus MCI	
	Mean thickness (SE)	Mean thickness (SE)	Mean thickness (SE)	*p-value	Mean difference (SE)	+p-value	Mean difference (SE)	+p-value	Mean difference (SE)	+p-value
Model 1										
Average, μm	72.73 (1.09)	73.73 (1.35)	77.79 (1.31)	**<0.001**	−5.06 (1.27)	**<0.001**	−4.06 (1.55)	**0.009**	−1.00 (1.50)	0.505
Superior sector, μm	72.66 (1.43)	73.48 (1.76)	77.65 (1.71)	**0.003**	−4.99 (1.66)	**0.003**	−4.17 (2.03)	**0.042**	−0.82 (1.96)	0.675
Superonasal sector, μm	75.85 (1.28)	76.86 (1.58)	80.93 (1.53)	**0.001**	−5.07 (1.49)	**0.001**	−4.07 (1.82)	**0.026**	−1.01 (1.75)	0.565
Inferonasal sector, μm	73.65 (1.27)	75.04 (1.57)	78.80 (1.52)	**0.001**	−5.15 (1.48)	**0.001**	−3.76 (1.81)	**0.039**	−1.38 (1.74)	0.428
Inferior sector, μm	70.61 (1.42)	70.87 (1.75)	76.83 (1.70)	**<0.001**	−6.21 (1.65)	**<0.001**	−5.95 (2.02)	**0.004**	−0.26 (1.95)	0.894
Inferotemporal sector, μm	72.25 (1.27)	72.89 (1.57)	77.51 (1.53)	**<0.001**	−5.26 (1.48)	**<0.001**	−4.62 (1.81)	**0.011**	−0.64 (1.75)	0.716
Superotemporal sector, μm	71.51 (1.28)	73.10 (1.58)	75.11 (1.53)	**0.016**	−3.59 (1.49)	**0.016**	−2.01 (1.82)	0.271	−1.58 (1.75)	0.367
Model 2										
Average, μm	71.69 (1.27)	72.44 (1.58)	76.21 (1.54)	**0.001**	−4.52 (1.35)	**0.001**	−3.78 (1.56)	**0.016**	−0.75 (1.56)	0.632
Superior sector, μm	70.88 (1.66)	71.89 (2.06)	75.68 (2.02)	**0.007**	−4.80 (1.76)	**0.007**	−3.79 (2.03)	0.064	−1.01 (2.03)	0.621
Superonasal sector, μm	75.38 (1.49)	76.75 (1.85)	80.36 (1.81)	**0.002**	−4.99 (1.58)	**0.002**	−3.62 (1.83)	**0.049**	−1.37 (1.83)	0.454
Inferonasal sector, μm	74.06 (1.49)	75.10 (1.85)	78.68 (1.81)	**0.004**	−4.63 (1.58)	**0.004**	−3.58 (1.83)	0.051	−1.04 (1.83)	0.569
Inferior sector, μm	68.90 (1.65)	68.01 (2.04)	73.83 (2.00)	**0.005**	−4.93 (1.75)	**0.005**	−5.83 (2.02)	**0.004**	0.89 (2.02)	0.659
Inferotemporal sector, μm	71.02 (1.48)	70.82 (1.83)	75.17 (1.80)	**0.009**	−4.16 (1.57)	**0.009**	−4.35 (1.81)	**0.017**	0.20 (1.81)	0.914
Superotemporal sector, μm	69.94 (1.49)	71.68 (1.84)	73.36 (1.80)	**0.031**	−3.42 (1.58)	**0.031**	−1.67 (1.82)	0.359	−1.75 (1.82)	0.338

SE, standard error *p-value represents the main effect by treating the three groups as a continuous variable; +p-value represents the pair-wise comparison between two groups Model 1: adjusted for age, gender, ethnicity and SD-OCT signal strength; Model 2: adjusted for age, gender, ethnicity, SD-OCT signal strength, hypertension, diabetes and history of myocardial infarction.

Table 3
Relationship of retinal nerve fiber layer (RNFL) thickness with Alzheimer's disease (AD) and mild cognitive impairment (MCI)

RNFL	AD ($n=92$)	MCI ($n=40$)	Controls ($n=123$)		AD versus Controls		MCI versus Controls		AD versus MCI	
	Mean thickness (SE)	Mean thickness (SE)	Mean thickness (SE)	*p-value	Mean difference (SE)	+p-value	Mean difference (SE)	+p-value	Mean difference (SE)	+p-value
Model 1										
Average, μm	86.83 (1.44)	89.21 (1.76)	90.37 (1.71)	**0.038**	−3.53 (1.70)	**0.038**	−1.15 (2.03)	0.57	−2.38 (1.98)	0.231
Superior quadrant, μm	105.7 (2.34)	110.9 (2.86)	113.5 (2.77)	**0.005**	−7.81 (2.75)	**0.005**	−2.64 (3.29)	0.423	−5.17 (3.21)	0.108
Nasal quadrant, μm	68.54 (1.60)	68.93 (1.96)	68.10 (1.90)	**0.815**	0.44 (1.88)	0.815	0.82 (2.25)	0.715	−0.39 (2.19)	0.861
Inferior quadrant, μm	108.2 (2.59)	112.2 (3.17)	114.3 (3.07)	**0.046**	−6.11 (3.05)	**0.046**	−2.07 (3.65)	0.57	−4.03 (3.55)	0.257
Temporal quadrant, μm	64.89 (1.89)	65.10 (2.30)	65.25 (2.23)	0.873	−0.36 (2.22)	0.873	−0.15 (2.65)	0.955	−0.21 (2.59)	0.936
Model 2										
Average, μm	85.89 (1.64)	87.00 (2.02)	87.51 (2.00)	0.365	−1.62 (1.78)	0.365	−0.50 (2.00)	0.801	−1.11 (2.02)	0.581
Superior quadrant, μm	105.1 (2.69)	109.1 (3.31)	111.1 (3.26)	**0.039**	−6.04 (2.92)	**0.039**	−2.06 (3.27)	0.529	−3.98 (3.30)	0.229
Nasal quadrant, μm	68.01 (1.83)	66.89 (2.26)	65.33 (2.22)	0.179	2.68 (1.99)	0.179	1.56 (2.23)	0.484	1.12 (2.25)	0.619
Inferior quadrant, μm	107.1 (2.96)	108.8 (3.65)	109.6 (3.60)	0.434	−2.52 (3.21)	0.430	−0.76 (3.60)	0.83	−1.76 (3.64)	0.630
Temporal quadrant, μm	63.23 (2.21)	63.29 (2.73)	63.54 (2.69)	0.896	−0.31 (2.40)	0.900	−0.25 (2.69)	0.93	−0.06 (2.72)	0.980

SE, standard error *p-value represents the main effect by treating the three groups as a continuous ordinal variable; +p-value represents the pair-wise comparison between two groups Model 1: adjusted for age, gender, ethnicity and SD-OCT signal strength; Model 2: adjusted for age, gender, ethnicity, SD-OCT signal strength, optic disc size, hypertension, diabetes and history of myocardial infarction.

Table 4
The area under the receiver operating characteristic curves (AUCs) of ganglion cell-inner plexiform layer (GC-IPL) and retinal nerve fiber layer (RNFL) thicknesses to discriminate Alzheimer's disease (AD), mild cognitive impairment (MCI), and AD/MCI from cognitively normal controls, adjusting for age and gender

	AD versus control		MCI versus controls		AD/MCI versus control	
	AUC	95% CI	AUC	95% CI	AUC	95% CI
GC-IPL thickness						
Average	0.658	(0.531–0.784)	0.661	(0.529–0.793)	0.659	(0.540–0.777)
Superior sector	0.602	(0.475–0.728)	0.642	(0.510–0.775)	0.614	(0.498–0.729)
Superonasal sector	0.589	(0.468–0.711)	0.623	(0.485–0.759)	0.599	(0.485–0.713)
Inferonasal sector	0.647	(0.515–0.780)	0.666	(0.539–0.793)	0.653	(0.536–0.769)
Inferior sector	0.722	(0.592–0.850)	0.674	(0.542–0.805)	0.707	(0.592–0.822)
Inferotemporal sector	0.685	(0.515–0.822)	0.688	(0.558–0.818)	0.686	(0.560–0.811)
Superotemporal sector	0.625	(0.508–0.741)	0.608	(0.475–0.742)	0.62	(0.507–0.732)
RNFL						
Average	0.601	(0.478–0.724)	0.608	(0.475–0.742)	0.597	(0.491–0.702)
Superior quadrant	0.596	(0.464–0.728)	0.556	(0.424–0.688)	0.584	(0.467–0.701)
Nasal quadrant	0.48	(0.352–0.607)	0.468	(0.341–0.595)	0.476	(0.363–0.590)
Inferior quadrant	0.64	(0.521–0.760)	0.609	(0.480–0.738)	0.631	(0.519–0.743)
Temporal quadrant	0.504	(0.385–0.622)	0.534	(0.410–0.659)	0.513	(0.406–0.620)

AUC, area under the receiver operating characteristic curve.

IPL and RNFL reduction), and using SD-OCT not only may help to improve the diagnostic accuracy for AD in the earliest stages, but also potentially track disease progression and detect neuroprotective effects of novel therapeutic agents in clinical trials. Recent reports have also used SD-OCT to assess RGC neuronal abnormalities in other neurodegenerative diseases such as multiple sclerosis and Parkinson's disease [39, 40]. Nevertheless, it is noted that SD-OCT can only assess a small part of the central nervous system, specifically that corresponding to the RGCs, even though neurodegenerative diseases tends to affect the central nervous system in a diffuse manner. Moreover, it is noteworthy that there is age-related reduction in RGCs and RGC axons in the normal retina [41, 42]. Thus, assessment of the RGC neuronal and axonal loss in AD should take into account the normal age-related loss of RGCs (age-related loss of GC-IPL is about $-0.3\,\mu$m/year) [41, 42]. Future studies including replication by different groups and more analyses using longitudinal data will be important to clarify the role of SD-OCT imaging in reflecting pathological neuronal loss in AD and MCI.

The strengths of this study include a large sample size of uniformly diagnosed AD and MCI patients, and comprehensive and objective assessment of RGC neuronal and optic nerve axonal loss using a commercial available SD-OCT modality. Our study has a number of limitations. First, due to the cross-sectional nature of our data, the causal and temporal relationships between GC-IPL and RNFL with MCI, AD cannot be examined. Second, cases and controls were selected from different study populations (hospital outpatient cases and population-based controls). Although both consisted of elderly Singaporeans, the control population was relatively younger and had only Chinese participants, which may have resulted in sampling bias and residual confounding. Nevertheless, the mean difference (4 to 5 μm) is larger than the expected age-related loss (age-related loss of GC-IPL is about $-0.3\,\mu$m/year) [41, 42]. Third, there may be residual confounding factors (e.g., depressive symptoms) that we have not controlled for that could bias or modify the associations observed in our sample. Fourth, presence of maculopathy (e.g., epiretinal membrane, diabetic macular edema, and age-related macular degeneration) might affect the measurement of retinal thickness. Nevertheless, we have examined all intra-retinal segmentation to confirm the accuracy of macular GC-IPL measurement.

In summary, reduction of macular GC-IPL is accompanied by reduction of perpapillary RNFL in AD, and is more strongly related to MCI. Retinal SD-OCT may provide a new noninvasive paradigm for quantitative evaluation of RGC neuronal and optic nerve axonal loss for assessing neurodegenerative disorders in AD and MCI, providing a potential new tool for identifying neuronal degeneration which may facilitate earlier intervention in AD and ultimately, the prevention of dementia.

ACKNOWLEDGMENTS

The study was supported by Academic Center of Excellence, GlaxoSmithKline (GSK) (100/019/550)

and National Medical Research Council (NMRC), Singapore (NMRC/STaR/0003/2008).

Authors' disclosures available online (http://j-alz.com/manuscript-disclosures/14-1659r2).

REFERENCES

[1] Vickers JC, Dickson TC, Adlard PA, Saunders HL, King CE, McCormack G (2000) The cause of neuronal degeneration in Alzheimer's disease. *Prog Neurobiol* **60**, 139-165.

[2] Devanand DP, Pradhaban G, Liu X, Khandji A, De Santi S, Segal S, Rusinek H, Pelton GH, Honig LS, Mayeux R, Stern Y, Tabert MH, de Leon MJ (2007) Hippocampal and entorhinal atrophy in mild cognitive impairment: Prediction of Alzheimer disease. *Neurology* **68**, 828-836.

[3] Hampel H, Frank R, Broich K, Teipel SJ, Katz RG, Hardy J, Herholz K, Bokde AL, Jessen F, Hoessler YC, Sanhai WR, Zetterberg H, Woodcock J, Blennow K (2010) Biomarkers for Alzheimer's disease: Academic, industry and regulatory perspectives. *Nat Rev Drug Discov* **9**, 560-574.

[4] Ikram MK, Cheung CY, Wong TY, Chen CP (2012) Retinal pathology as biomarker for cognitive impairment and Alzheimer's disease. *J Neurol Neurosurg Psychiatry* **83**, 917-922.

[5] London A, Benhar I, Schwartz M (2013) The retina as a window to the brain-from eye research to CNS disorders. *Nat Rev Neurol* **9**, 44-53.

[6] Blanks JC, Hinton DR, Sadun AA, Miller CA (1989) Retinal ganglion cell degeneration in Alzheimer's disease. *Brain Res* **501**, 364-372.

[7] Hinton DR, Sadun AA, Blanks JC, Miller CA (1986) Optic-nerve degeneration in Alzheimer's disease. *N Engl J Med* **315**, 485-487.

[8] Sadun AA, Bassi CJ (1990) Optic nerve damage in Alzheimer's disease. *Ophthalmology* **97**, 9-17.

[9] Hedges TR, 3rd, Perez Galves R, Speigelman D, Barbas NR, Peli E, Yardley CJ (1996) Retinal nerve fiber layer abnormalities in Alzheimer's disease. *Acta Ophthalmol Scand* **74**, 271-275.

[10] Tsai CS, Ritch R, Schwartz B, Lee SS, Miller NR, Chi T, Hsieh FY (1991) Optic nerve head and nerve fiber layer in Alzheimer's disease. *Arch Ophthalmol* **109**, 199-204.

[11] Drexler W, Fujimoto JG (2008) State-of-the-art retinal optical coherence tomography. *Prog Retin Eye Res* **27**, 45-88.

[12] Huang D, Swanson EA, Lin CP, Schuman JS, Stinson WG, Chang W, Hee MR, Flotte T, Gregory K, Puliafito CA, et al (1991) Optical coherence tomography. *Science* **254**, 1178-1181.

[13] Parisi V, Restuccia R, Fattapposta F, Mina C, Bucci MG, Pierelli F (2001) Morphological and functional retinal impairment in Alzheimer's disease patients. *Clin Neurophysiol* **112**, 1860-1867.

[14] Berisha F, Feke GT, Trempe CL, McMeel JW, Schepens CL (2007) Retinal abnormalities in early Alzheimer's disease. *Invest Ophthalmol Vis Sci* **48**, 2285-2289.

[15] Iseri PK, Altinas O, Tokay T, Yuksel N (2006) Relationship between cognitive impairment and retinal morphological and visual functional abnormalities in Alzheimer disease. *J Neuroophthalmol* **26**, 18-24.

[16] Lu Y, Li Z, Zhang X, Ming B, Jia J, Wang R, Ma D (2010) Retinal nerve fiber layer structure abnormalities in early Alzheimer's disease: Evidence in optical coherence tomography. *Neurosci Lett* **480**, 69-72.

[17] Paquet C, Boissonnot M, Roger F, Dighiero P, Gil R, Hugon J (2007) Abnormal retinal thickness in patients with mild cognitive impairment and Alzheimer's disease. *Neurosci Lett* **420**, 97-99.

[18] Kesler A, Vakhapova V, Korczyn AD, Naftaliev E, Neudorfer M (2011) Retinal thickness in patients with mild cognitive impairment and Alzheimer's disease. *Clin Neurol Neurosurg* **113**, 523-526.

[19] Kromer R, Serbecic N, Hausner L, Froelich L, Aboul-Enein F, Beutelspacher SC (2014) Detection of retinal nerve fiber layer defects in Alzheimer's disease using SD-OCT. *Front Psychiatry* **5**, 22.

[20] Koh VT, Tham YC, Cheung CY, Wong WL, Baskaran M, Saw SM, Wong TY, Aung T (2012) Determinants of ganglion cell-inner plexiform layer thickness measured by high-definition optical coherence tomography. *Invest Ophthalmol Vis Sci* **53**, 5853-5859.

[21] Mwanza JC, Durbin MK, Budenz DL, Sayyad FE, Chang RT, Neelakantan A, Godfrey DG, Carter R, Crandall AS (2012) Glaucoma diagnostic accuracy of ganglion cell-inner plexiform layer thickness: Comparison with nerve fiber layer and optic nerve head. *Ophthalmology* **119**, 1151-1158.

[22] American Psychiatric Association (1994) *Diagnostic and Statistical Manual of Mental Disorders*, American Medical Association, Washington DC.

[23] McKhann GM, Knopman DS, Chertkow H, Hyman BT, Jack CR, Jr., Kawas CH, Klunk WE, Koroshetz WJ, Manly JJ, Mayeux R, Mohs RC, Morris JC, Rossor MN, Scheltens P, Carrillo MC, Thies B, Weintraub S, Phelps CH (2011) The diagnosis of dementia due to Alzheimer's disease: Recommendations from the National Institute on Aging-Alzheimer's Association workgroups on diagnostic guidelines for Alzheimer's disease. *Alzheimers Dement* **7**, 263-269.

[24] Petersen RC, Smith GE, Waring SC, Ivnik RJ, Kokmen E, Tangelos EG (1997) Aging, memory, and mild cognitive impairment. *Int Psychogeriatr* **9** Suppl 1, 65-69.

[25] Cheung CY, Chen D, Wong TY, Tham YC, Wu R, Zheng Y, Cheng CY, Saw SM, Baskaran M, Leung CK, Aung T (2011) Determinants of quantitative optic nerve measurements using spectral domain optical coherence tomography in a population-based sample of non-glaucomatous subjects. *Invest Ophthalmol Vis Sci* **52**, 9629-9635.

[26] Lavanya R, Jeganathan VS, Zheng Y, Raju P, Cheung N, Tai ES, Wang JJ, Lamoureux E, Mitchell P, Young TL, Cajucom-Uy H, Foster PJ, Aung T, Saw SM, Wong TY (2009) Methodology of the Singapore Indian Chinese Cohort (SICC) eye study: Quantifying ethnic variations in the epidemiology of eye diseases in Asians. *Ophthalmic Epidemiol* **16**, 325-336.

[27] Sahadevan S, Lim PP, Tan NJ, Chan SP (2000) Diagnostic performance of two mental status tests in the older chinese: Influence of education and age on cut-off values. *Int J Geriatr Psychiatry* **15**, 234-241.

[28] Leung CK, Cheung CY, Weinreb RN, Qiu Q, Liu S, Li H, Xu G, Fan N, Huang L, Pang CP, Lam DS (2009) Retinal nerve fiber layer imaging with spectral-domain optical coherence tomography: A variability and diagnostic performance study. *Ophthalmology* **116**, 1257-1263, 1263 e1251-1252.

[29] Mwanza JC, Oakley JD, Budenz DL, Chang RT, Knight OJ, Feuer WJ (2011) Macular ganglion cell-inner plexiform layer: Automated detection and thickness reproducibility with spectral domain-optical coherence tomography in glaucoma. *Invest Ophthalmol Vis Sci* **52**, 8323-8329.

[30] Liu M, Duggan J, Salt TE, Cordeiro MF (2011) Dendritic changes in visual pathways in glaucoma and other neurodegenerative conditions. *Exp Eye Res* **92**, 244-250.

[31] Gasparini L, Crowther RA, Martin KR, Berg N, Coleman M, Goedert M, Spillantini MG (2011) Tau inclusions in retinal ganglion cells of human P301S tau transgenic mice: Effects on axonal viability. *Neurobiol Aging* **32**, 419-433.

[32] Parnell M, Guo L, Abdi M, Cordeiro MF (2012) Ocular manifestations of Alzheimer's disease in animal models. *Int J Alzheimers Dis* **2012**, 786494.

[33] Curcio CA, Allen KA (1990) Topography of ganglion cells in human retina. *J Comp Neurol* **300**, 5-25.

[34] Blanks JC, Torigoe Y, Hinton DR, Blanks RH (1996) Retinal pathology in Alzheimer's disease. I. Ganglion cell loss in foveal/parafoveal retina. *Neurobiol Aging* **17**, 377-384.

[35] Williams PA, Thirgood RA, Oliphant H, Frizzati A, Littlewood E, Votruba M, Good MA, Williams J, Morgan JE (2013) Retinal ganglion cell dendritic degeneration in a mouse model of Alzheimer's disease. *Neurobiol Aging* **34**, 1799-1806.

[36] Marziani E, Pomati S, Ramolfo P, Cigada M, Giani A, Mariani C, Staurenghi G (2013) Evaluation of retinal nerve fiber layer and ganglion cell layer thickness in Alzheimer's disease using spectral-domain optical coherence tomography. *Invest Ophthalmol Vis Sci* **54**, 5953-5958.

[37] Weiner MW, Aisen PS, Jack CR, Jr., Jagust WJ, Trojanowski JQ, Shaw L, Saykin AJ, Morris JC, Cairns N, Beckett LA, Toga A, Green R, Walter S, Soares H, Snyder P, Siemers E, Potter W, Cole PE, Schmidt M, Alzheimer's Disease Neuroimaging I (2010) The Alzheimer's disease neuroimaging initiative: Progress report and future plans. *Alzheimers Dement* **6**, 202-211 e207.

[38] Blennow K, de Leon MJ, Zetterberg H (2006) Alzheimer's disease. *Lancet* **368**, 387-403.

[39] Ratchford JN, Saidha S, Sotirchos ES, Oh JA, Seigo MA, Eckstein C, Durbin MK, Oakley JD, Meyer SA, Conger A, Frohman TC, Newsome SD, Balcer LJ, Frohman EM, Calabresi PA (2013) Active MS is associated with accelerated retinal ganglion cell/inner plexiform layer thinning. *Neurology* **80**, 47-54.

[40] Garcia-Martin E, Satue M, Fuertes I, Otin S, Alarcia R, Herrero R, Bambo MP, Fernandez J, Pablo LE (2012) Ability and reproducibility of Fourier-domain optical coherence tomography to detect retinal nerve fiber layer atrophy in Parkinson's disease. *Ophthalmology* **119**, 2161-2167.

[41] Leung CK, Ye C, Weinreb RN, Yu M, Lai G, Lam DS (2013) Impact of age-related change of retinal nerve fiber layer and macular thicknesses on evaluation of glaucoma progression. *Ophthalmology* **120**, 2485-2492.

[42] Leung CK, Yu M, Weinreb RN, Ye C, Liu S, Lai G, Lam DS (2012) Retinal nerve fiber layer imaging with spectral-domain optical coherence tomography: A prospective analysis of age-related loss. *Ophthalmology* **119**, 731-737.